 CMC, vol.26, no.1, pp.19-35, 2011

Frequency Shift Curve Based Damage Detection Method for Beam Structures

Y. Zhang[1,2] **and Z.H. Xiang**[1,3]

Abstract: Vibration based damage detection methods play an important role in the maintenance of beam structures such as bridges. However, most of them require the accurate measurement of structural mode shapes, which may not be easily satisfied in practice. Since the measurement of frequencies is more accurate than that of mode shapes, this paper proposes a frequency shift curve (FSC) method, based on the equivalence between the FSC due to auxiliary mass and the mode shape square, which has been demonstrated to be effective in structural damage detection. Two damage indices based on the FSC are developed, which are called the local outlier detection index and the global outlier detection index, respectively. The efficiency and reliability of the proposed method are demonstrated by numerical simulations and experimental results. Compared with traditional methods, this method can provide reliable results without the requirement of fixing many sensors on the structure.

Keywords: damage detection, frequency shift curve, beam, auxiliary mass

1 Introduction

Vibration based damage detection methods have been widely studied for decades as global damage detection techniques [Carden and Fanning (2004); Alvandi and Cremona (2006); Doebling *et al.* (1998); Farrar (2001); Fan and Qiao (2011); Hu, Wang, Fukunaga *et al.* (2001)]. Almost all these methods are based on the structural dynamic properties, such as natural frequencies, mode shapes and damping. Pandey *et al.* proposed the mode shape curvature (MSC) method [Pandey *et al.* (1991)], and the flexibility matrix (FM) method [Pandey and Biswas (1994)]. The MSC method was used for the identification of delamination [Hu, Fukunaga,

[1] AML, Department of Engineering Mechanics, Tsinghua University, Beijing, 100084, China
[2] Corresponding author: Z.H. Xiang, Tel.: +86-10-62796873; Fax. +86-10-62772902. *Email address*: xiangzhihai@tsinghua.edu.cn
[3] Southwest University of Science and Technology, Mianyang, 621010, China

Kameyama *et al*. (2002)], which is a well-known damage in laminated materials, such as CFRP laminates [Hu, Sekine, Fukunaga *et al.* (1999)]. Stubbs *et al*. (1992) proved that the strain energy method is effective on locating damages. Wang *et al.* proposed a combination method using the test data of static deformation and natural frequencies [Wang *et al.* (2001)]. Fukunaga *et al.* proposed a method only using the data in frequency domain to locate the damage and evaluate the damage extent, which, however, preliminarily needs an additional database relating the change of the data in frequency domain to the damage position [Fukunaga *et al.* (2002)]. Based on the MSC and the FM, Zhang and Aktan (1995) defined another damage index based on the flexibility curvature.

Although the validities of aforementioned methods have been demonstrated by numerical simulations and laboratory experiments in many literatures, it seems that they all require high quality mode shapes. However, with the existing modal testing methods, no matter using the forced vibration or the ambient vibration, the measurement accuracy of mode shapes is not as ideal as that of natural frequencies. In addition, many sensors have to be fixed on the structure during the testing and a certain eigenvalue or singular value problem has to be solved. These could be troublesome for onsite measurement. To solve this problem, Zhong *et al*. (2008) used the derivative of highly accurate natural frequencies due to auxiliary mass to detect damage. However, only numerical simulations were presented in that paper. And the numerical error of derivatives calculated by the difference method could seriously affect its performance in practice.

Another inconvenience of many traditional damage detection methods is the requirement of comparing the dynamic properties of the damaged structure with those of its intact status, which may not be always available in practice. To circumvent this problem, Ratcliffe (1997) proposed a gapped smoothing method (GSM) using modified Laplacian operator on the mode shape curvature. Then, Yoon *et al*. (2009) extended the GSM and suggested a global fitting method (GFM).

Inspired by the method proposed by Zhong *et al*. (2008), we still want to use the natural frequencies due to auxiliary mass to detect damage, because these frequencies can be accurately measured without requiring densely fixing sensors on the structure. For this purpose, this paper firstly obtains the analytical formulation of the distribution of natural frequencies due to auxiliary mass over the beam, which is called the frequency shift curve (FSC). Based on this formulation, we can easily identify the equivalence between the FSC and the mode shape square, which has been proven to be very effective on structural damage detection [Fang and Perera (2009)]. Then two damage indices based on the FSC and the modified GSM and GFM are proposed, which use neither the information of intact structures nor the difference method to get the derivative. Finally, both numerical simulations and

experiments have been conducted to demonstrate the effectiveness of this method.

The following text is organized as: Section 2 presents the theoretical explanation of the equivalence between the mode shape square and the FSC by an interaction model of an Euler-Bernoulli beam and a spring-mass system. Based on this analysis, a local and a global index are proposed for damage detection. Section 3 gives some numerical examples to validate this explanation and shows the potential of these indices for damage detection. Section 4 gives experimental results for further demonstration. Finally, conclusions and discussions are presented in Section 5.

2 Theoretical analysis

The auxiliary mass fixed on a beam structure will change the natural frequencies of the system and the frequency shift curve could be illustrated to be equivalent to the mode shape square. Based on this, two damage indices can be proposed.

2.1 The interaction between an Euler-Bernoulli beam and a spring-mass system

A model of Euler-Bernoulli beam with a spring-mass system is shown in Fig.1. In this model, the mass M is supported on a spring of large stiffness k at position x_0. This beam has bending stiffness EI and mass $\bar{m}$ in unit length. For simplicity, some practical factors such as damping are temporarily ignored here. However, we can show later by experiments that these factors do not have crucial influence on damage detection results.

The governing equations of the beam and the spring-mass system can be written as:

$$\bar{m}\ddot{u}(x,t) + EIu''''(x,t) = f(t)\,\delta(x - x_0) \tag{1}$$

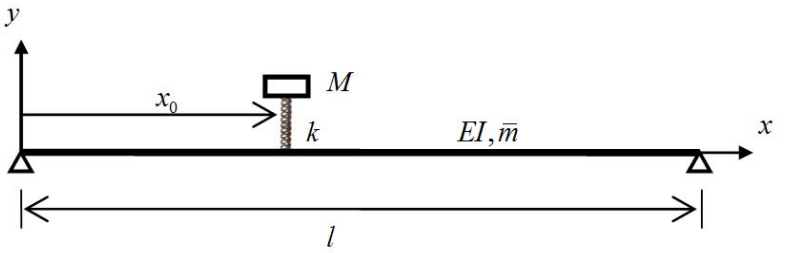

Figure 1: The interaction between an Euler-Bernoulli beam and a spring-mass system

$$M\ddot{q}(t)+kq(t)=ku(x_0,t) \tag{2}$$

where $q(t)$ and $u(x,t)$ are the vertical displacements of the mass and the beam measured from the static equilibrium position, respectively; $u''''=\frac{\partial^4 u}{\partial x^4}$, $\ddot{u}=\frac{\partial^2 u}{\partial t^2}$, $\ddot{q}=\frac{\partial^2 u}{\partial t^2}$; δ is the Dirac delta function and $f(t)\delta(x-x_0)$ is the contact force between the mass and the beam; and

$$f(t)=-M(g+\ddot{q}) \tag{3}$$

Using the modal superposition method, the beam displacement can be represented as:

$$u(x,t)=\sum_n \phi_n(x)\,q_n(t) \tag{4}$$

where $\phi_n(x)$ is the nth mode shape of the beam and $q_n(t)$ is the corresponding modal coordinate.

Substituting Eq. (4) into Eq. (1), multiplying $\phi_m(x)$ on both sides and integrating over the whole beam, obtains:

$$\int_0^l \bar{m}\phi_m \sum_n \phi_n \ddot{q}_n(t)\,\mathrm{d}x+\int_0^l EI\phi_m \sum_n \phi''''_n\, q_n(t)\mathrm{d}x=\int_0^l \phi_m f(t)\,\delta(x-x_0)\,\mathrm{d}x \tag{5}$$

When the stiffness of the spring k is large enough, the displacement of the mass could be approximately represented as:

$$q(t)\approx u(x_0,t)=\sum_n \phi_n(x_0)\,q_n(t) \tag{6}$$

Substituting Eqs. (3) and (6) into Eq. (5), and noting the orthogonal property of mode shapes, Eq. (5) becomes:

$$\left[1+\frac{M}{\Phi}\phi_n^2(x_0)\right]\ddot{q}_n+\omega_{bn}^2 q_n=-M\frac{g+\sum\limits_{i\neq n}\ddot{q}_i\phi_i(x_0)}{\Phi}\phi_n(x_0) \tag{7}$$

where ω_{bn} is the nth natural frequency of the beam; and Φ_n is an integration constant:

$$\Phi_n=\int_0^l \varphi_n^2(x)\,\mathrm{d}x \tag{8}$$

Thus, the natural frequencies of the whole system, including the beam and the spring-mass system, can be approximately written as:

$$\omega_n^2(x_0)=\frac{\omega_{bn}^2}{1+\frac{M}{\Phi_n}\varphi_n^2(x_0)} \tag{9}$$

From the above relation, one can define the nth FSC as:

$$\Omega_n(x) = \frac{1}{\omega_{bn}^2} + \frac{\frac{M}{\Phi_n}\varphi_n^2(x_0)}{\omega_{bn}^2} \tag{10}$$

According to Eq. (10), it is easy to find that the nth FSC could contain all dynamic information in the mode shape square $\phi_n^2(x)$.

2.2 Two new damage indices

Similar to the power mode shape curvature [Fang and Perera (2009)], the curvature of the nth FSC (CFSC) of the damaged beam structure at each measurement point x_i could be calculated by using the central difference method:

$$\kappa_{i,n}^d = \left(\Omega_n^d(x_i)\right) \approx \frac{\Omega_n^d(x_{i-1}) - 2\Omega_n^d(x_i) + \Omega_n^d(x_{i+1})}{l_i^2} \tag{11}$$

where l_i is the distance between two measurement points and superscript $d$denotes the damaged state. For intact structures, the $\kappa_{i,n}^d$ should be smoothly changed along the beam length. While for damaged structures, the $\kappa_{i,n}^d$ will have an abrupt change at the damaged location. Therefore, the curve of $\kappa_{i,n}^d$ could be used to locate the damage theoretically. However, owing to the numerical errors introduced by the central difference method, the identified damage information could not be very reliable. To solve this problem, this paper proposes two indices similar to the GSM [Ratcliffe (1997)] and the GFM [Yoon *et al.* (2009)] for damage detection. These indices can be constructed by the local or global information of the $\kappa_{i,n}^d$ curve, as explained in following.

2.2.1 Local outlier detection index

Instead of directly taking the central difference result in (11), we can get a better interpolation of the curvature of the nth CFSC at position x_i, denoted as $C_{\kappa n}(x_i)$, according to its adjacent values as:

$$C_{\kappa n}(x_i) = c_{0,\kappa n} + c_{1,\kappa n}x_i + c_{2,\kappa n}x_i^2 + c_{3,\kappa n}x_i^3 \tag{12}$$

where the coefficients $c_{0,\kappa n}$, $c_{1,\kappa n}$, $c_{2,\kappa n}$ and $c_{3,\kappa n}$ are determined by $\kappa_{i-2,n}^d$, $\kappa_{i-1,n}^d$, $\kappa_{i+1,n}^d$ and $\kappa_{i+2,n}^d$. For boundary points, i.e. x_1 and x_2, the coefficients are determined by $\kappa_{2,n}^d$, $\kappa_{3,n}^d$, $\kappa_{4,n}^d$, $\kappa_{5,n}^d$ as well as $\kappa_{1,n}^d$, $\kappa_{3,n}^d$, $\kappa_{4,n}^d$, $\kappa_{5,n}^d$ respectively. In fact, the cubic polynomial in (12) is the Lagrange interpolating polynomial determined by the four

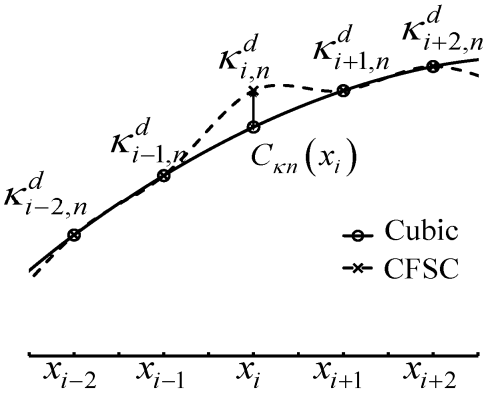

Figure 2: The CFSC and calculated cubic polynomial at point x_i

nearest CFSC points. Fig. 2 shows the CFSC and the calculated cubic polynomial at point x_i.

Based on the CFSC and its cubic interpolation, the nth local outlier detection index (LODI) is defined as:

$$\delta_{Ln}(x_i) = \frac{\left(C_{\kappa n}(x_i) - \kappa^d_{i,n}\right)^2}{\max_i \left[\left(C_{\kappa n}(x_i) - \kappa^d_{i,n}\right)^2\right]} \tag{13}$$

When N ($N > 1$) modes are considered, we can use the combined LODI

$$\delta_L = \frac{1}{N}\sum_{n=1}^{N} \delta_{Ln} \tag{14}$$

and normalize it by its maximum value.

2.2.2 Global outlier detection index

The CFSC can also be fitted globally by using a polynomial $p_n(x)$ of degree S_n:

$$p_n(x) = \sum_{i=0}^{S_n} p_{i,n} x^i \tag{15}$$

The optimum S_n can be iteratively determined as follows:

Let $S_n = 3$ at the beginning;

Construct a Vandermonde matrix based on the location coordinates $\mathbf{x} = [x_i]^{\mathrm{T}}$:

$$V_n = \begin{bmatrix} x_1^{S_n} & x_1^{S_n-1} & \cdots & 1 \\ x_2^{S_n} & x_2^{S_n-1} & \cdots & 1 \\ \cdots & & & \cdots \\ x_T^{S_n} & x_T^{S_n} & \cdots & 1 \end{bmatrix} \tag{16}$$

where T denotes the number of measurement points.

Decompose the Vandermonde matrix $\mathbf{V}_n$ into an upper triangular matrix $\mathbf{R}_n$ and an orthogonal matrix $\mathbf{Q}_n$:

$$\mathbf{V}_n = \mathbf{Q}_n \cdot \mathbf{R}_n \tag{17}$$

If the condition number of $\mathbf{R}_n$ is less than a pre-specified threshold, say 1×10^{10} in this paper, let $S_n = S_n + 1$ and go to step (2). Otherwise, stop.

With the optimumS_n, the coefficients $p_{i,n}$ can be easily obtained:

$$[p_{S_n,n}, p_{S_n-1,n}, \cdots, p_{0,n}]^{\mathrm{T}} = \mathbf{V}_n^{-1} \cdot \Omega_n^d(\mathbf{x}) = \mathbf{R}_n^{-1} \cdot \mathbf{Q}^{\mathrm{T}} \cdot \Omega_n^d(\mathbf{x}) \tag{18}$$

Fig. 3 shows the nth CFSC and globally fitted polynomial $p_n(x)$, from which the global outlier detection index (GODI) can be defined as:

$$\delta_{Gn}(x_i) = \frac{\left[p_n(x_i) - \kappa_{i,n}^d\right]^2}{\max_i \left\{\left[p_n(x_i) - \kappa_{i,n}^d\right]^2\right\}} \tag{19}$$

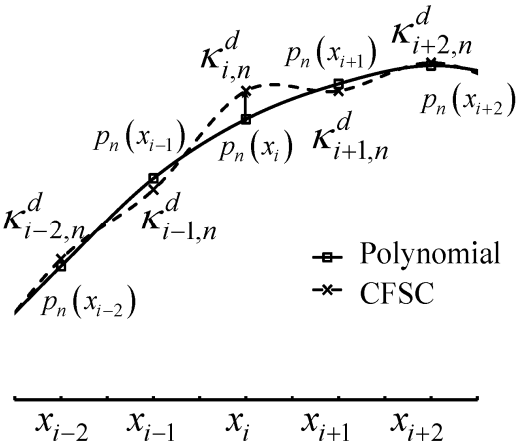

Figure 3: The nth CFSC and calculated polynomial $p_n(x)$

When N ($N > 1$) modes are considered, we can use the combined GODI

$$\delta_G = \frac{1}{N}\sum_{n=1}^{N}\delta_{Gn} \tag{20}$$

and normalize it by its maximum value.

3 Numerical examples

In this section, numerical examples of a simply supported beam are presented to firstly check the validity of Eq. (10), and then to demonstrate the potential of the damage indices proposed in Section 2. All these simulations are conducted by the Linear Perturbation Frequency Package in the ABAQUS finite element software.

3.1 The equivalence between the FSC and the mode shape square

An interaction system with a simply-support beam and a spring-mass system with $M = 500\text{kg}$ and $k = 1\times10^{11}\text{N / m}$ is adopted to verify the equivalence between the FSC and the mode shape square. The beam has the cross-sectional area $A = 0.5\text{m}^2$, the moment of inertia $I = 0.014\text{m}^4$, the length $l = 10\text{m}$, the elastic modulus $E = 70\text{GPa}$, and the density $\rho = 2700\text{kg / m}^3$.

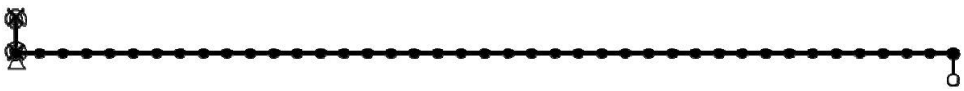

Figure 4: The FEM model of the interaction of a beam and a spring-mass system

As Fig. 4 shows, during the simulation, the beam is equally divided into 40 two-dimensional beam elements; and the spring-mass system moves along the beam node by node. At each node, the natural frequencies of the whole system can be easily calculated. Thus, obtains the FSCs numerically. Then, as Fig. 5 shows, we can compare the numerical FSCs with the ones calculated by Eq. (10). It observes that the maximum relative error between the numerical and the analytical FSCs is less than 1%. This proves the validity of Eq. (10). In addition, since the FSC is a linear function of $\varphi_n^2(x)$ (refer to Eq. (10)), the normalized FSC should be equivalent to $\varphi_n^2(x)$, which has been proved to be very effective on structural damage detection [Fang and Perera (2009)].

3.2 Damage detection based on two indices

Both single and multiple damage scenarios are considered to study the effectiveness of the proposed damage indices. In single damage scenario, elements 13 and 14

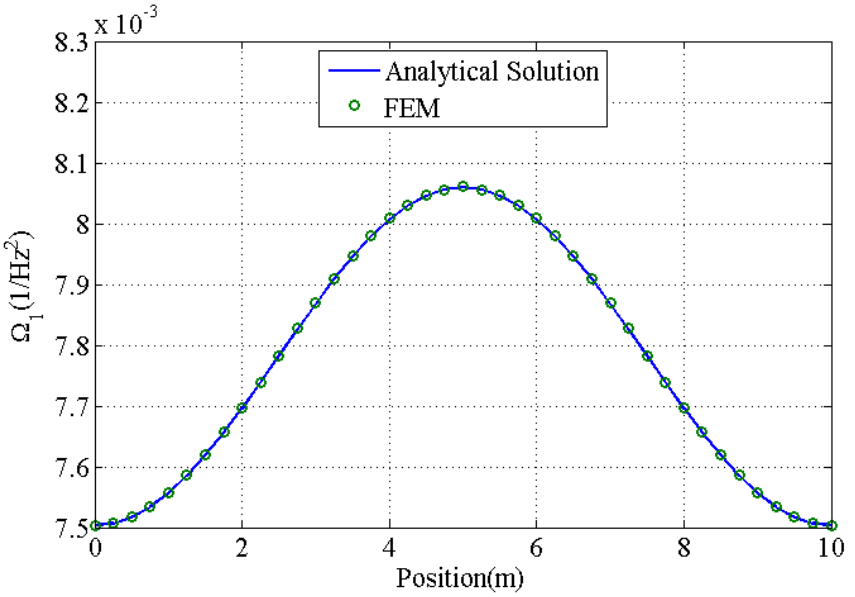

(a) The first mode

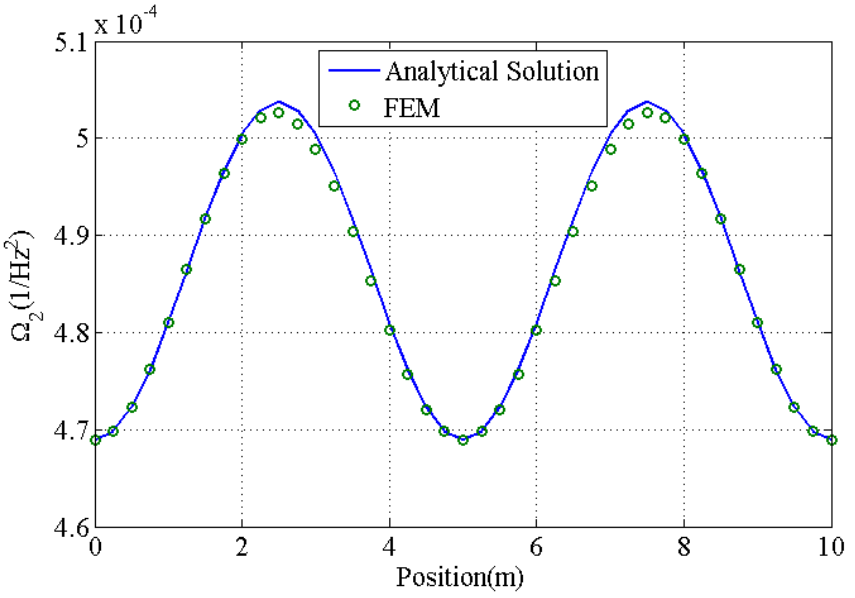

(b) The second mode

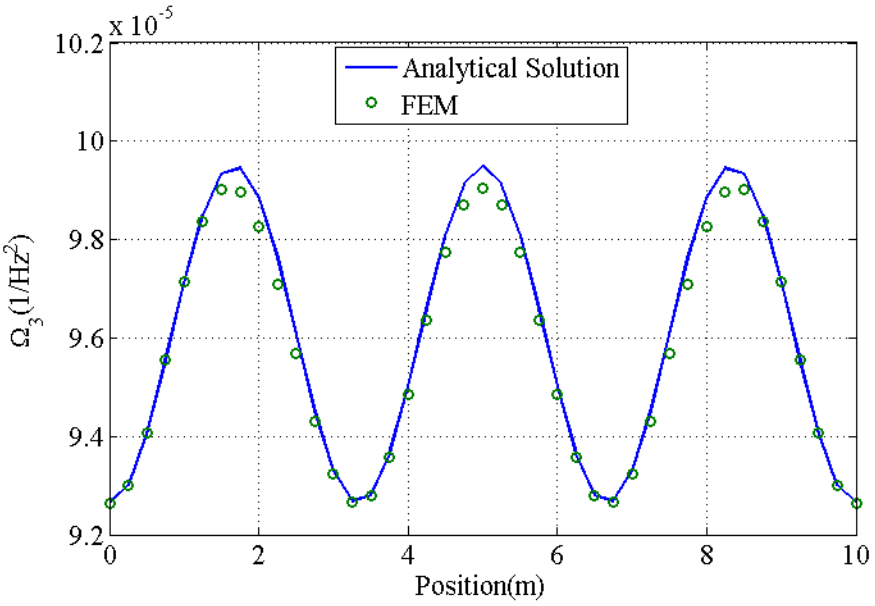

(c) The third mode

Figure 5: The first three FSCs

(3m-3.5m away from the left end of the beam) are regarded as the damaged region with 20% reduction in height. In multiple damage scenario, elements 13, 14 and element 23 (5.5m-5.75m away from the left end of the beam) are regarded as the damaged regions with 20% reduction in height.

Fig. 6 plots the LODIs of the first two modes for the single damage scenario. From this plot, one can clearly identify the peak value at the damaged region, although there are some noises nearby. However, these noises can be greatly suppressed if we use the combined LODI.

Fig. 7 plots the GODIs of the first two modes for the single damage scenario. Compared with Fig. 6, we can easily conclude that the GODIs can clearly identify the damage with fewer noises.

Fig. 8 plots the LODIs of the first two modes for the multiple damages scenario. It observes that the first damage (elements 13 and 14) can be successfully identified by a clear peak at that position no matter using only mode 1, mode 2 or their combination; while there are two peaks near the second damage (element 23) if only use mode 1. All in all, it seems that the combined LODI can give more reliable

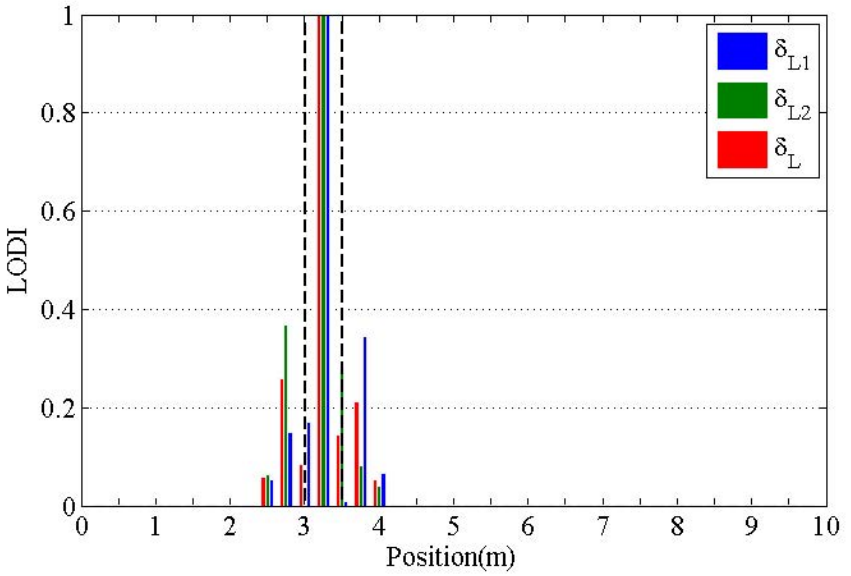

Figure 6: Single damage detected by the LODI

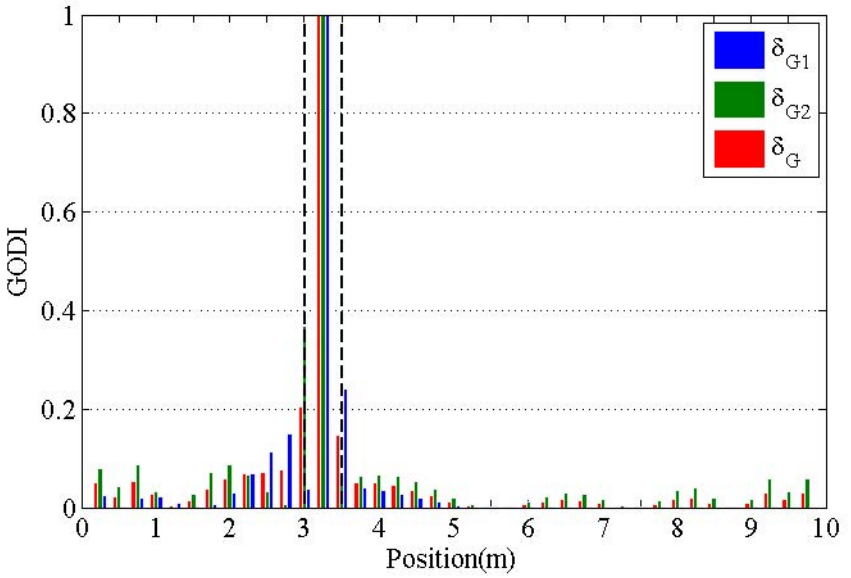

Figure 7: Single damage detected by the global outlier detection operator

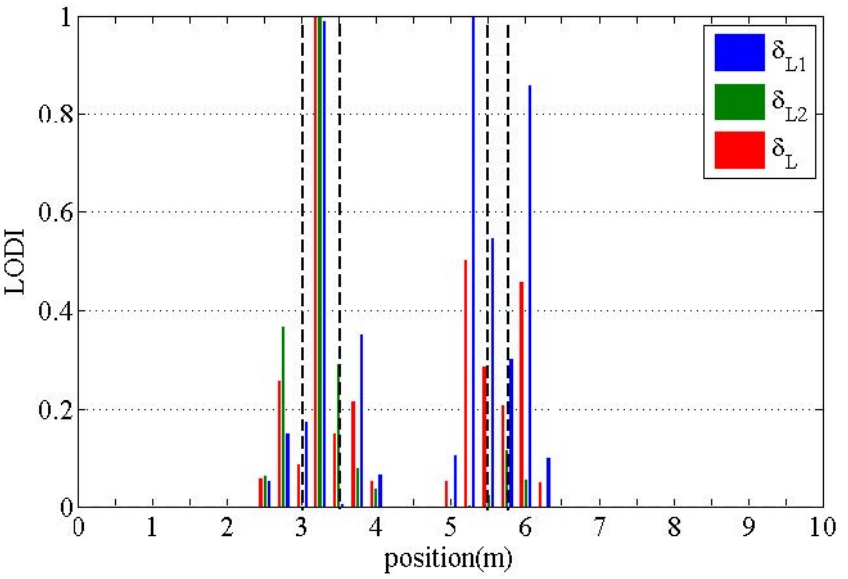

Figure 8: Multiple damages detected by the LODI

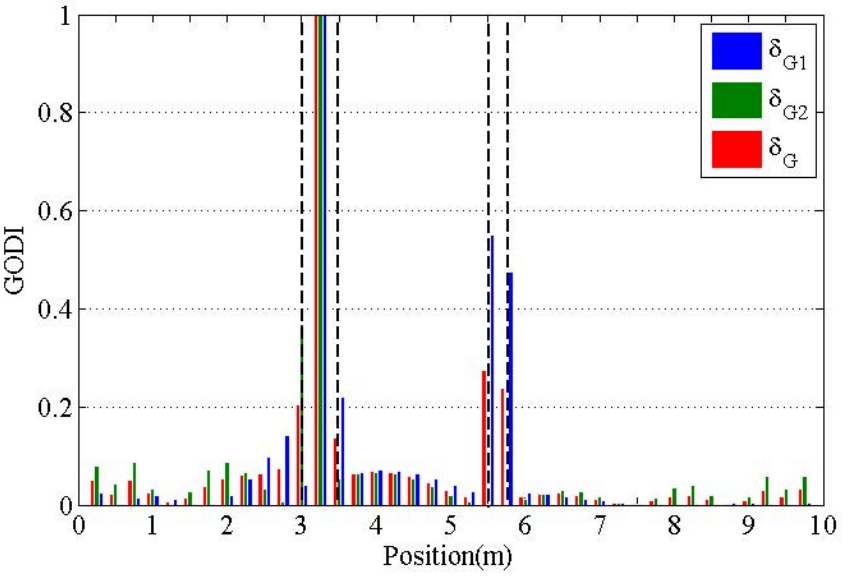

Figure 9: Multiple damages detected by the GODI

damage information.

Fig. 9 plots the GODIs of the first two modes for the multiple damages scenario. It observes that although the GODI using mode 2 fails to identify the second damage, the GODI using mode 1 shows better performance than the LODI: both two damages are indicated by clear peaks and the amplitude at the first damage is as twice high as that at the second damage. In addition, similar to the LODI, the GODI using the combination of mode 1 and mode 2 looks more reliable.

4 Experimental verification

With the confidence obtained in numerical simulations, a simple experiment was carried out to give further verification for these proposed indices.

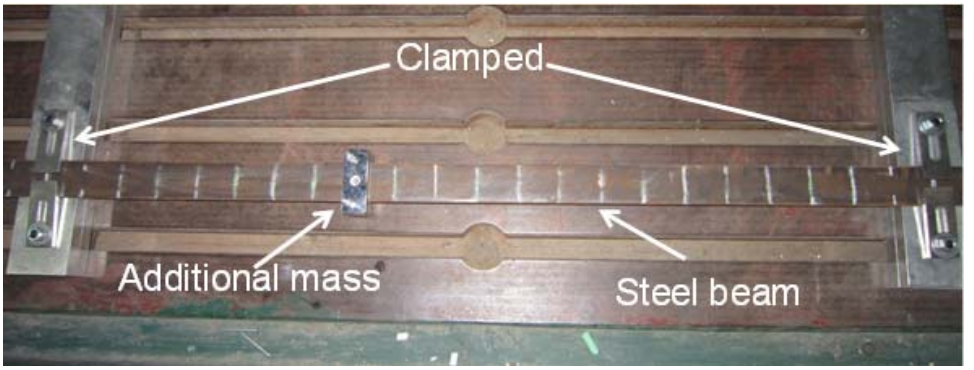

Figure 10: The photograph of the tested beam

4.1 The experiment setup

The photograph of a thin steel beam in dimension of 1200mm×30mm×4.5mm is shown in Fig 10. This beam was clamped with the span of 1000mm and 19 nodes were marked on the beam at the uniform interval of 50mm. A single damage of 20mm in width produced by reducing the height to 4mm was located at 350mm away from the left end. A 500g auxiliary mass could be clamped at different positions of the beam (shown in Fig 11).

During the experiment, the auxiliary mass moved node by node from the left end to the right end. At each node, the free vibration response of the beam was recorded by an accelerometer fixed on the auxiliary mass. From these signals, the natural frequencies of the whole system were calculated by the FFT method.

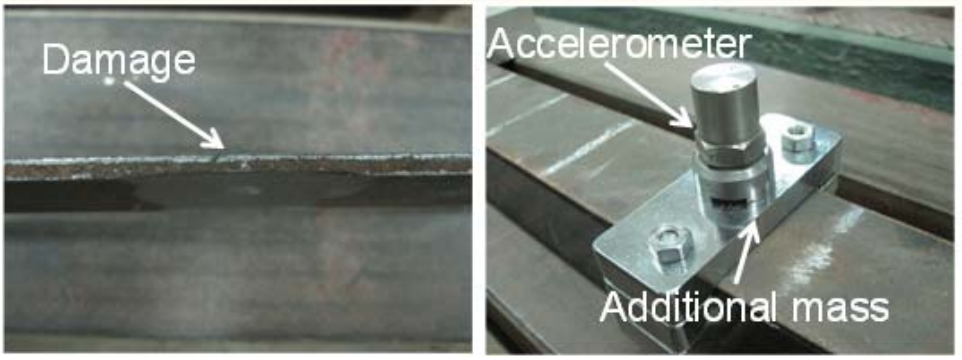

Figure 11: The photograph of the damage and additional mass

4.2 Experimental results

The first two natural frequencies of the mass-beam system were measured when the mass moved on the beam node by node. Then the two damage indices were used to detect the single damage, which are plotted in Fig. 12 and Fig. 13.

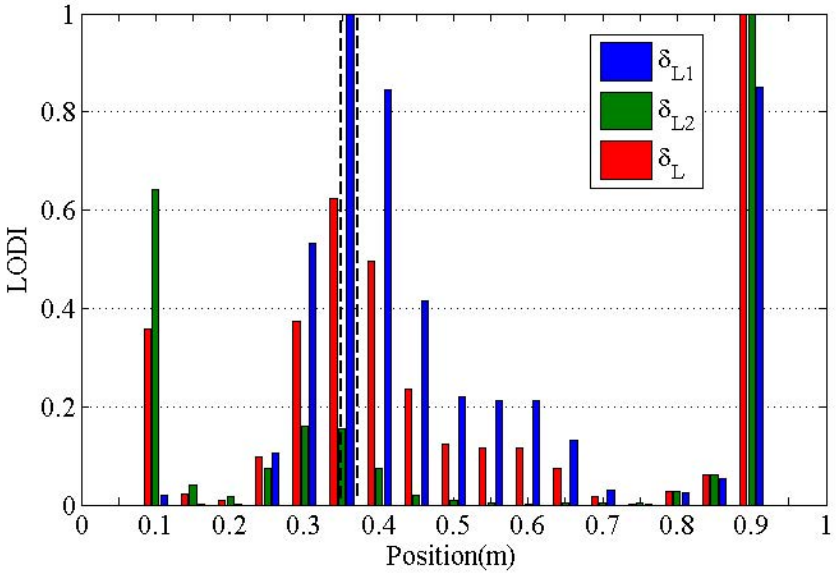

Figure 12: The damage detected by the LODI

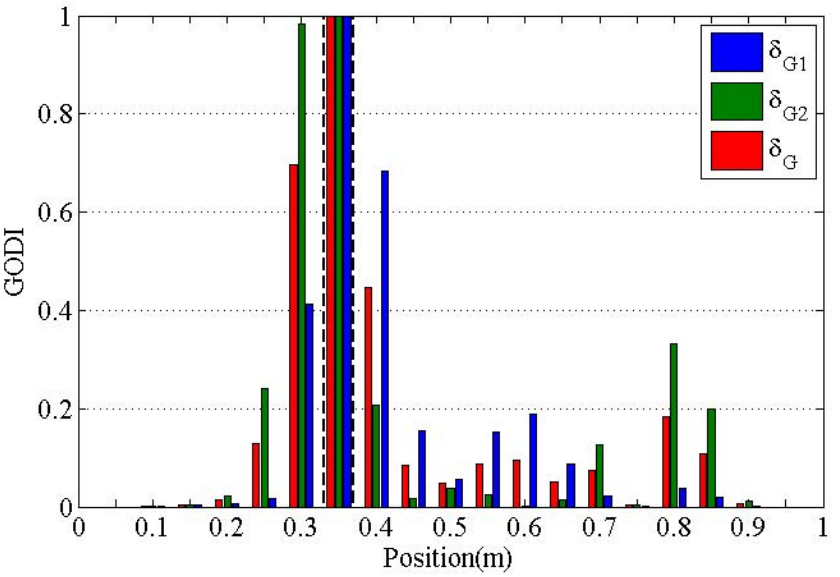

Figure 13: The damage detected by the GODI

From Fig. 12 and Fig. 13, it observes that both indices could detect the damage with a clear peak at the damaged position. However, similar to the conclusion drawn in numerical simulations, the GODI shows better performance than the LODI, because the amplitudes of the LODIs are exceptionally high at the boundary nodes, which are false indications of damage. This is probably because the cubic polynomial values at boundary nodes are determined by only one side of $\kappa_{i,n}^{d}$. In addition, contrary to the observations in numerical simulations, the indices using mode 1 can give better result than those using mode 2 or the combination of mode 1 and mode 2. This is probably because the lower frequency could be measured more accurately in the experiment.

5 Discussion and conclusion

Based on a simple theoretical model, this paper firstly demonstrates the equivalence between the FSC and the mode shape square. This is the foundation that ensures the success of damage detection from the change of the FSC. In addition, Eq. (10) implies that the FSC could be more sensitive to the mode shape square (contains the damage information) if the mass M is heavier. However, since the theoretical analysis is based on linear equations, the mass M should not be too heavy to produce large deformations.

To avoid the adverse influence of the numerical errors produced by the central difference method, two damage indices are proposed based on the change of locally interpolated or globally fitted CFSC. Both numerical simulations and experimental results demonstrate the validity of these two indices. However, it seems that the boundary effect would affect the detection accuracy of the LODI, while the GODI usually gives better results.

All in all, the proposed damage detection method can be easily implemented in practice, because it uses only the frequency due to auxiliary mass, which can be accurately measured with a single accelerator.

Acknowledgement: This work is support by National Science Foundation of China with grant number 10802040). This support is gratefully acknowledged. Many thanks also go to Professor Qiuhai Lu and Doctor Bo Wang for their valuable help in preparing the experiment.

References

Alvandi, A.; Cremona, C. (2006): Assessment of vibration-based damage identification techniques. *Journal of sound and vibration*, vol. 292, pp. 179-202.

Carden, E.P.; Fanning, P. (2004): Vibration based condition monitoring: a review. *Structural Health Monitoring*, vol.3, pp. 355-377.

Doebling, S.W.; Farrar, C.R.; Prime, M.B.. (1998): A summary review of vibration-based damage identification methods. *Shock and Vibration Digest*, vol. 30, pp. 91-105.

Fan, W.; Qiao, P.Z. (2011): Vibration-based Damage Identification Methods: A Review and Comparative Study. *Structural Health Monitoring*, vol.10, pp. 83-111.

Fang, S.E.; Perera, R. (2009): Power mode shape for early damage detection in linear structures. *Journal of Sound and Vibration*, vol. 324, pp. 40-56.

Farrar, C.R. (2001): Vibration-based structural damage identification. *Philosophical Transactions of the Royal Society: Mathematical, Physical & Engineering Sciences*, vol. 359, pp. 131–149.

Fukunaga, H; Hu, N.; Chang, F.K. (2002): Structural damage identification using piezoelectric sensors. *International Journal of Solids and Structures*, vol. 39, pp. 393-418.

Hu, N.; Wang, X.; Fukunaga, H.; Yao, Z.H.; Zhang, H.X.; Wu, Z.S. (2001): Damage assessment of structures using modal test data. *International Journal of Solids and Structures*, vol. 38, pp. 3111-3126.

Hu, N.; Fukunaga, H.; Kameyama, M.; Aramaki, Y.; Chang, F.K. (2002):

Vibration analysis of delaminated composite beams and plates using a higher-order finite element. *International Journal of Mechanical Sciences*, vol. 44, pp. 1479-1503.

Hu, N.; Sekine, H.; Fukunaga, H.; Yao, Z.H. (1999): Impact analysis of composite laminates with multiple delaminations. *International Journal of Impact Engineering*, vol. 22, pp. 633-648.

Kim, C.Y.; Jung, D.S.; Kim, N.S.; Kwon, S.D.; Feng, M.Q. (2003): Effect of vehicle weight on natural frequencies of bridges measured from traffic-induced vibration. *Earthquake Engineering and Engineering Vibration*, vol. 2, pp. 109-115.

Law, S.S.; Zhu, X.Q. (2004): Dynamic behavior of damaged concrete bridge structures under moving vehicular loads. *Engineering Structures*, vol. 26, pp. 1279-1293.

Pandey, A.K.; Biswas, M.; Samman, M.M. (1991): Damage detection from changes in curvature mode shapes. *Journal of sound and vibration*, vol. 145, pp. 321-332.

Pandey, A.K.; Biswas, M. (1994): Damage detection in structures using changes in flexibility. *Journal of Sound and Vibration*, vol. 169, pp. 3–17.

Ratcliffe, C.P. (1997): Damage detection using a modified Laplacian operator on mode shape data. *Journal of Sound and Vibration*, vol. 204, pp. 505-517.

Stubbs, N.; Kim, J.T.; Topole, K. (1992): An efficient and robust algorithm for damage localization in offshore platforms. *Proceedings of the ASCE 10th Structures Congress*, pp. 543-546.

Wang, X.; Hu, N.; Fukunaga, H.; Yao, Z.H. (2001): Structural damage identification using static test data and changes in frequencies. *Engineering Structures*, vol. 23, pp. 610-621.

Yang, Y.B.; Lin, C.W.; Yau, J.D. (2004): Extracting bridge frequencies from the dynamic response of a passing vehicle. *Journal of Sound and Vibration*, vol. 272, pp. 471-493.

Yoon, M.K.; Heider, D.; Gillespie, J.W.; Ratcliffe, C.P.; Crane, R.M. (2009): Local damage detection with the global fitting method using mode shape data in notched beams. *Journal of Nondestructive Evaluation*, vol. 28, pp. 63-74.

Zhang, Z.; Aktan, A.E. (1995): The damage indices for constructed facilities. *Proceedings of the IMAC*, vol. 13, pp. 1520–1529.

Zhong, S.C.; Oyadiji, S.O.; Ding K. (2008): Response-only method for damage detection of beam-like structures using high accuracy frequencies with auxiliary mass spatial probing. *Journal of Sound and Vibration*, vol. 311, pp. 1075-1099.